

ENGINE SYSTEM LOADS ANALYSIS COMPARED TO HOT-FIRE DATA

Greg Frady*, John M. Jennings†, Katherine Mims‡, Joseph Brunty#, Ph.D.
NASA George C. Marshall Space Flight Center
Huntsville, Alabama

Eric R. Christensen†, Ph.D.
SAIC Inc.
Huntsville, Alabama

Abstract

Early implementation of structural dynamics finite element analyses for calculation of design loads is considered common design practice for high volume manufacturing industries such as automotive and aeronautical industries. However, with the rarity of rocket engine development programs starts, these tools are relatively new to the design of rocket engines. In the NASA MC-1 engine program, the focus was to reduce the cost-to-weight ratio. The techniques for structural dynamics analysis practices were tailored in this program to meet both production and structural design goals. Perturbation of rocket engine design parameters resulted in a number of MC-1 load cycles necessary to characterize the impact due to mass and stiffness changes. Evolution of loads and load extraction methodologies, parametric considerations and a discussion of load path sensitivities are important during the design and integration of a new engine system. During the final stages of development, it is important to verify the results of an engine system model to determine the validity of the results. During the final stages of the MC-1 program, hot-fire test results were obtained and compared to the structural design loads calculated by the engine system model. These comparisons are presented in this paper.

1.0 Introduction

The MC-1 engine (Figure 1), also referred to as the FASTRAC engine, is a 60,000-pound thrust liquid oxygen/kerosene (LOX/RP-1) engine designed and developed at the NASA Marshall Space Flight Center (MSFC). The engine uses a single-stage, gas-generator cycle with one turbopump, a single-use combustion chamber and bell shaped nozzle. The nozzle uses a composite ablative liner within a

composite overwrap. The MC-1 engine was planned for use in the X-34 technology testbed vehicle.

A number of nozzles were utilized during the development including 15:1 area ratio nozzles for ground testing and 30:1 nozzles for altitude. In addition to the area ratio differences in the hot fire testing were different materials. Some nozzles were made from a fiber-glass material while others were made from a carbon-based composite material. Both had significantly different characteristics, but the results presented in this paper are based upon the carbon-based material.

The X-34 technology testbed demonstration vehicle (Figure 2) was a NASA program intended to demonstrate key technologies applicable to the Reusable Launch Vehicle (RLV) Program¹. The objective of the X-34 was flight demonstration of key reusable launch vehicle operations and technologies directed at the RLV goal of low-cost space access. Key technologies included composite primary and secondary airframe structures, composite reusable propellant tanks, cryogenic insulation and propulsion system elements, advanced thermal protection systems and materials, low-cost avionics, integrated vehicle health monitoring systems, and flush air data systems. The X-34 vehicle is a winged vehicle with a wing span of 27.7 feet and a length of 58.3 feet. In a typical X-34 flight, the testbed vehicle would be dropped from an L-1011 aircraft at 30,000 feet, the engine would start and accelerate the vehicle to Mach 8. The vehicle would climb to 250,000 feet, followed by a coast phase, re-entry and horizontal landing on a conventional runway.

An engine system model was constructed of the MC-1 engine to generate loads for the components and interfaces. Engine components and interfaces analyzed included items such as ducts, brackets,

*Dynamics Engineer, Structural Dynamics/Loads Group ED21, AIAA Member

‡Dynamics Engineer, Structural Dynamics/Loads Group ED21, AIAA Member

§Dynamics Engineer, Structural Dynamics/Loads Group ED21, AIAA Member

#Dynamics Group Lead, Structural Dynamics/Loads Group ED21, AIAA Member

†Senior Systems Engineer, SAIC Inc., AIAA Associate Member

gimbals, gimbal actuators, etc. The analysis utilized a finite element model (FEM) of the engine system including all major components and vehicle interfaces. The engine was tested at the Boeing/Rocketdyne ALPHA 1 Test Facility. The FEM of the engine system included the stiffness of the facility feedlines, actuator attach points, and included both the 15:1 and 30:1 nozzle configurations. Test data was obtained using strain gages and accelerometers and then compared to stress analyses performed at MSFC. Comparisons were made for the predicted modes, frequencies, and accelerations calculated by the engine system FEM.

This paper describes the work done at MSFC to simulate the structural dynamic response of the MC-1 engine system and how it correlated to hot-fire data. The primary purpose of this analysis was to calculate the predicted dynamic loads on engine components and interfaces for use in component stress analysis and design during engine development. This was done to reduce risk and testing delays due to preventable integration failures, and to reduce cost.

2.0 Finite Element (FE) System Model Construction

The main components of the engine system FEM consist of the nozzle, the manifold assembly, the turbopump and gas generator, the ducts, the brackets, and the vehicle interfaces. The model, pictured in Figure 3, was constructed using MSC/NASTRAN and MSC/PATRAN software. The model was constructed using design drawings and electronic engine assembly geometry files for alignment and construction of duct and bracket models. During design iterations, new electronic files were provided along with the dimensional drawings for the purpose of incorporating design modifications into the model. Descriptions of each of the major engine component models created are given below.

2.1 Chamber/Nozzle and Manifold Assembly

The chamber/nozzle, shown in Figure 4, is composed of two main composite layers with several metallic inserts and over-bands. The 30:1 nozzle is 74 inches long with a weight of approximately 500 lbs. The inner layer is composed of composite tape wrapped at an angle from the global longitudinal axis, and this layer is then overwrapped with a composite tape that is wound in a helical pattern. For several reasons, which are explained in detail in Ref. 2, the model of

this structure for dynamic analysis required the use of composite plate elements rather than solid elements. To use these elements, the independent material properties of each layer of the composite lay-up had to be obtained for the element coordinate system. The properties required were the Young's modulus in the element axial direction, the Young's modulus in the circumferential direction, the shear modulus, and Poisson's ratio. Since the nozzle contour varies substantially along its length and the tape was wound at two wrap angles, the material properties in the element coordinate system were different for each axial row of elements. Furthermore, the overwrap was wound at a continually varying wind angle and therefore the overwrap material properties in the element coordinate system also vary with axial position. Substantial coordinate transformations were required to obtain these properties from those obtained during material testing. This was accomplished by first using a FORTRAN program to read the wrap angle, wind angle, and cone angle for each axial row of elements, as calculated using a detailed spreadsheet incorporating the design geometry information. The derived transformations from the original tested properties were then used to calculate the plate element material properties. These properties were written to a material property card specifically for each element row and were then copied directly into the finite element data deck for modal analysis.

The nozzle model described above was modified when nozzle modal test data became available. This was done by adjusting the engineering constants such that calculated frequencies matched those measured from tests. The resulting scale factors varied from 0.65 for the tangential Young's modulus to 1.5 for the shear modulus. These scale factors were extrapolated for different nozzle ratios. For more details on the modal correlation of the nozzle, see Ref. 2.

The manifold assembly is a very stiff, nearly rigid structure constructed of steel. This structure contains the main injector plate and the engine gimbal supports. It is modeled with QUAD4 and CTRIA3 plate elements.

2.2 Turbopump and Gas Generator

In the Load Cycle 1 model, the gas generator was modeled as an equivalent beam and the turbopump was modeled as a rigid mass. This rigid mass was connected to the turbopump brackets and the ducts via rigid link elements. A flexible beam or "stick" model for the turbopump was added in load cycle 3.

A solid 3D model of the turbine housing was also created and used to calculate the housing modes and natural frequencies. The turbopump beam model cross-sectional properties were then modified to tune the beam model with the first few modes and frequencies of the housing model. This tuned stick turbopump model has been used in load cycles 3-9.

2.3 Ducts and Brackets

The propellant ducts have circular cross-sections and were modeled using beam elements. For straight portions of the ducts CBEAM elements were used since these portions of the ducts behave according to simple beam theory. In the curved sections and the elbows, however, the CBEND element is used. In these portions of the pipe, radial stress parallel to the radius of curvature will develop when the pipe bends and will cause the cross-section to deform into an oval shape which creates transverse stresses not present in a straight section of tube³. Therefore a 2D stress field is present within the pipe bend. This effect is included in the MSC/NASTRAN CBEND element.

The brackets used to attach components to the engine were modeled as elastic springs. The spring constants were determined by building a detailed 3D model of each bracket and calculating the displacements due to unit loads applied in the appropriate direction (see Figure 3).

2.4 Vehicle Interfaces

The interfaces between the engine system and the X-34 vehicle consist of the gimbal attachment, two gimbal actuators, and the feedline ducts. The actuators are attached to the engine using "belly bands" around the nozzle and are modeled as beams pinned at each end. At each of the interfaces the vehicle stiffness is modeled as a grounded elastic spring. The spring constants were calculated by the vehicle contractor and were determined from a finite element model with unit loads applied at the appropriate locations.

3.0 Loads and Environments

Initially, there were six load cases to be considered in the dynamic analysis. Those load cases included handling, lifting, and transportations loads, separation transient loads, start up and shutdown transient loads, steady state operation loads, re-entry loads, and landing loads, (Ref. 4). During the engine development program, there was one area where

comparisons between the dynamic analysis and ground tests could be performed. This area was steady state operation, which included quasi-static, sinusoidal, and random vibration loads for ground tests.

Steady State Operation

Two types of dynamic environments are induced by the operation of the engine itself. The first dynamic environment is due to the sinusoidal acceleration resulting from the rotation of the turbopump. The peak acceleration for the major frequency components of one, three, and six times pump synchronous operating speed were estimated and used. These loads were applied at the turbopump cg with a $\pm 10\%$ bandwidth about the excitation frequency.

The second dynamic environment resulting from the operation of the engine is the random acceleration due to sources in the turbopump, the gas generator, the combustion chamber, etc. The levels of random acceleration were determined using test data from the MA5 engine, which is similar in design to the MC-1 engine. An initial random vibration spectrum was obtained by scaling and enveloping the peak responses obtained from the test data. The resulting environments were detailed in Ref. 4.

In addition to the dynamic loads, during steady state operation there are also quasi-static applied loads due to vehicle acceleration (Ref. 4), engine gimbal acceleration, and 60,000 lb static thrust load. The steady-state sideload (Ref. 5) was also applied to the system. This load was conservatively assumed to be the same magnitude as the startup/shutdown sideloads.

4.0 Results

Summaries of the analysis results for load cycles 1-9 as well as a detailed description of the analysis methodology are given in References 4 and 6. The results presented show where the engine system model predicted very favorable modal analysis results and where the engine system model was hampered due to short-falls in methodological approaches to engine system random vibration analyses.

The MC-1 engine hot-fire test data provided a tremendous amount of insight into the capabilities of the engine system loads FEM developed for this program. The results answered a number of questions generated by the stress analysts and provided insight

into the modal characteristics of the engine throughout the engine burn. Since the engine's backbone structure consisted of the composite nozzle, it was important that the nozzle be tested and correlated separately and then integrated into the engine system model⁷. This showed some interesting results. The nozzle stiffness changed as the nozzle increased in temperature due to the hot gas flow during engine operation. As the engine burned during the first 60 seconds, the primary and secondary modes of the nozzle dropped in frequency. Figure 5 demonstrates that the nozzle modes shifted up to 30% the first 60 seconds with little change thereafter. Figures 6 and 7 illustrates the reason why there is movement in the with the modulus in the normal direction of the fibers having the largest influence in determining the changing dynamic characteristics of the nozzle. As temperatures continued to increase beyond 500 degrees F, the modes did not appreciably change apparently because the normal-direction elasticity had reached a saturation point due to a potential debonding in the local fibers.

Since the frequencies of the nozzle changed with time, it is reasonable to believe that the loads would also shift due to changing material characteristics during a hot-fire test. Figure 8 shows how the static loads shift as the engine burns. This was helpful to the stress analysts, and explained one of the reasons they saw a drift in the static strain data as the hot fire test continued.

The gas generator acceleration data, Figure 9, shows how this phenomenon affected other components of the engine. The data shows a very rough 60 seconds of firing and then a transition where the g's associated with the gas generator component quiets down by an order of magnitude less than it was during the first 60 seconds. It was even observed that the sound of the engine changed at 60 seconds into the burn.

Since the components of the engine were mounted on the nozzle bellyband, as shown in Figure 1, any stiffness changes of the nozzle were reflected in the engine components. As the nozzle stiffness changed, the load paths throughout the engine changed as well. During design iterations, it was discovered that the loads shifted somewhat proportionately, Figure 8, increasing in one area while decreasing in others as component modifications were performed. Figure 10 also shows an example of this sensitivity due to a simple wall thickness change in the exhaust duct. In addition to the load path sensitivity due to the nozzle properties, there was an additional fact that there

were no bellows in this engine. The loads were distributed throughout the various engine components making the stiff ducts act similar to stiff mounted brackets. Loads change significantly because of these stiffness sensitivities in some areas due to the change in the integrated stiffness of the entire engine.

There were other, more mixed results in the analysis of the MC-1 Engine analysis. The sinusoidal analysis had only one source, the turbopump, which gave satisfactory results while the random vibration environments were assumed to emanate from three primary sources, turbopump, gas generator, and combustion chamber. The large mass method⁸ was used to calculate the sinusoidal vibration loads for this engine system analysis using NASTRAN.

The large mass method was also used to calculate a part of the random vibration loads from a component perspective. For other components, Miles' equation⁹ was used to derive conservative random vibration loads. It was hoped that the MC-1 engine program would provide insight into the development of new random vibration engine system loads analysis techniques that would improve on the conservatism of component analysis methods that have been in use for many years. In the course of the program, the conservatism of the older methods were realized while demonstrating the validity of using engine system models to design many of the components of a new engine system. More detailed information as to how the response was calculated due to the random vibration environments is described in Ref. 4.

The dynamic characteristics of the model closely predicted the major modes of the engine system. Figures 11 through 15 illustrate how well the analytical results corresponded with data collected during hot-fire. In many cases, the modes were just slightly different from that of the actual hardware.

5.0 Conclusions

The model correlated very well with hot fire data due mostly to a correlated nozzle model and the approach taken to model the brackets and their stiffnesses. The model correlated well with modes and frequencies along with various g levels across the engine. Much of the correlation can be attributed to the nozzle correlation that was performed during the hot-fire testing. Another important feature in model correlation was the method used for modeling the bracket stiffnesses. The time taken to model the brackets as 3-D models was relatively short due to the

availability of 3-D geometry and the ease of importing that geometry into PATRAN for modeling.

A shortfall in methodologies caused some trouble with random vibration loads. This caused one component to have extremely high loads and negative margins through analysis, while test data proved otherwise. There was some skepticism concerning some of the high loads in the MC-1 engine program, but there was also a confidence that the engine could survive the mission it was called upon to perform. With higher design loads, came higher margins that can often cause unnecessary weight to be added to vehicle programs, but in many cases help an engine fulfill its function for a longer and more robust life.

High g's levels are nothing new to rocket engine analyses. They have become a trademark to a large degree. Significant work is currently in progress to determine how to lower the g-levels as well as the loads to make them more realistic and predictable during engine development programs. Work is also being performed to lower the environments to a more realistic level. Further, work is being performed on methodologies to help remove some of the pseudo-static motion that causes such high g-levels and loads during the analysis using the methodologies available in most finite element programs. Work is being performed to match the response of the engine rather than use the response as the engine excitation. All of these challenges are important and will be beneficial to some degree in developing new engine methodologies. However, history has shown the conservatism built into engine design practices have led to fairly low strains and stresses throughout many of the great rocket engine programs throughout the past few decades. One has to consider the cost associated with being more "accurate" in developing the design loads and wonder if new problems due to lower margins are going to haunt us in future programs as we move forward in this difficult area of engine loads development.

An excellent engine model was developed for the MC-1 program that explained many issues that arose during development testing. In many cases, the engine model probably prevented some hardware failures due to the fact that the engine was analyzed as a system before it was ever tested as a system. Due to the simplicity of the design, it provided excellent insight into the basic principles of engine development, which are very useful in extrapolating those ideas and principles to larger, more complex engines. The technologies of today have provided the capabilities to build complex engine models, but there

is still work to be performed in developing engine system loads and then deciding how best to use those loads to build a better, longer life engine.

6.0 References

1. D. C. Freeman, T. A. Talay and R. E. Austin, "The NASA Reusable Launch Vehicle Technology Program", Presented at the Space '96 Conference: 5th International Conference and Exposition on Engineering, Construction, and Operations in Space, Albuquerque, New Mexico, June 5, 1996.
2. Brown, A.M, and Sullivan, R.M, "Dynamic Modeling and Correlation of the X-34 Composite Rocket Nozzle", 1998 JANNAF Rocket Nozzle Technology Meeting, Salt Lake City, Utah, March 16-20, 1998.
3. R. Frick, "Determining Tube Stress From CBEND Element Forces and Moments", Presented at the MSC 1993 World User's Conference, Paper No. 64, May 1993.
4. Christensen, E., Frady, G., Mims, K., Brown, A., "Structural Dynamic Analysis of the X-34 Rocket Engine", paper no. 98-2012 presented at the 39th AIAA Structures, Structural Dynamics, and Materials Conference, April 20-23, 1998, Long Beach, CA.
5. P.N. Fuller, "J-2S Nozzle Side-Load Study", Rocketdyne Engineering Final Report Contract NAS8-25156, August 1972.
6. Frady, G., Christensen, E., Mims, K., Harris, D., Parks, R., Brunty, J., "Engine System Loads Development For The Fastrac 60K Flight Engine," paper no. 00-1612 presented at the 41th AIAA Structures, Structural Dynamics, and Materials Conference, April 3-6, 2000, Atlanta, GA.
7. Brown, A.M., "Temperature-Dependent Modal Test/Analysis Correlation of X-34 FASTRAC Composite Rocket Nozzle," submitted for the 2000 AIAA Structures, Structural Dynamics, and Materials Conference, April 3-6, 2000, Atlanta, GA.
8. P. Leger, I.M. Ide, and P. Paultre, "Multiple-Support Seismic Analysis of Large Structures",

Computers and Structures, Vol. 36, No. 6, pp. 1153-1158, 1990.

9. J. Miles, "On Structural Fatigue Under Random Loading", *Journal of Aeronautical Sciences*, Vol. 21, No. 11, Nov. 1954, pp. 753-762.

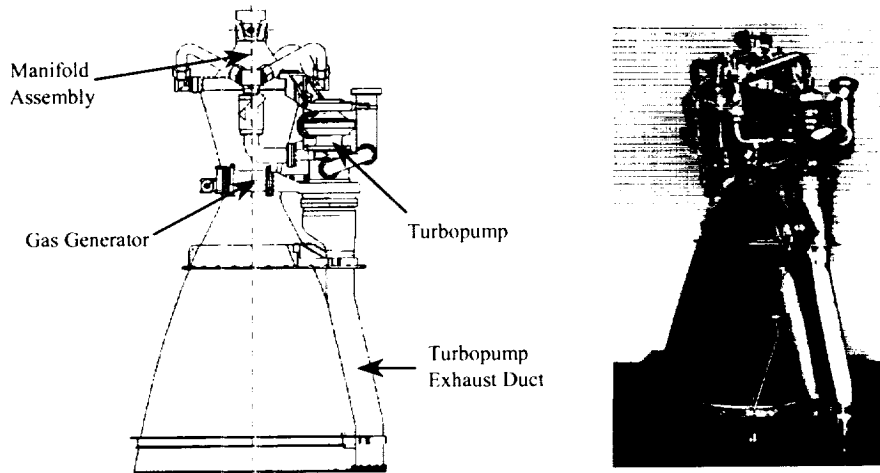


Figure 1. Fastrac 60K Engine



Figure 2. X-34 Vehicle

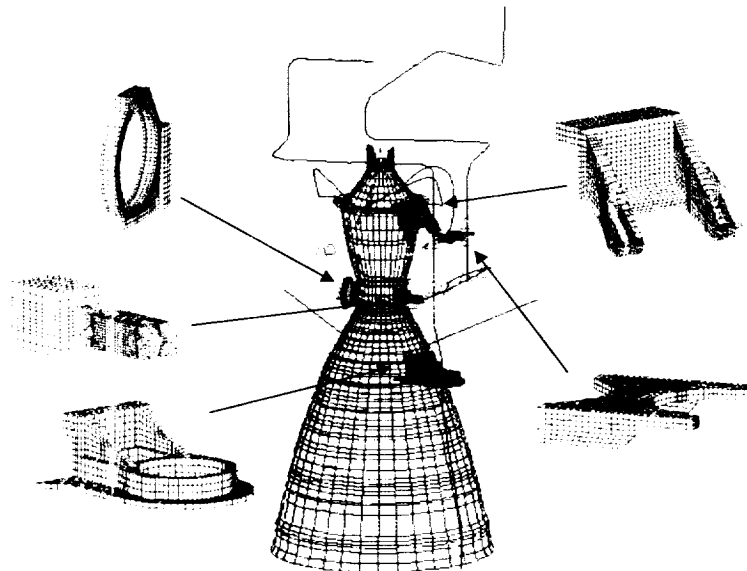


Figure 3. Engine System Dynamic FE Model

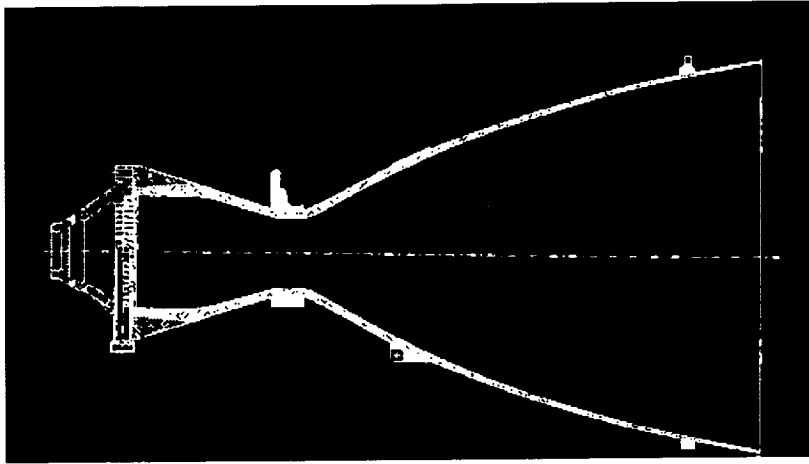


Figure 4. Composite Chamber/Nozzle

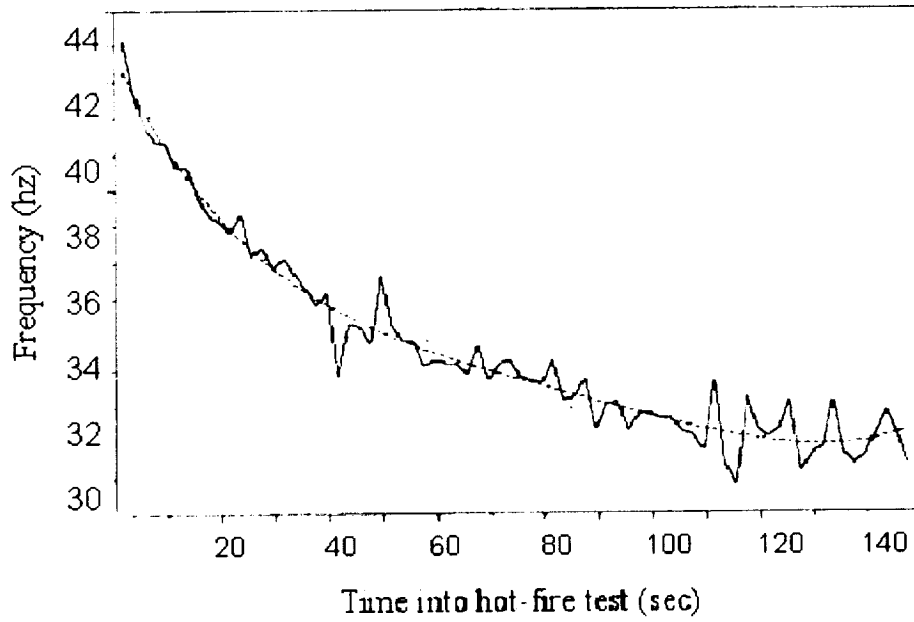


Figure 5. Modes Shift During Engine Burn

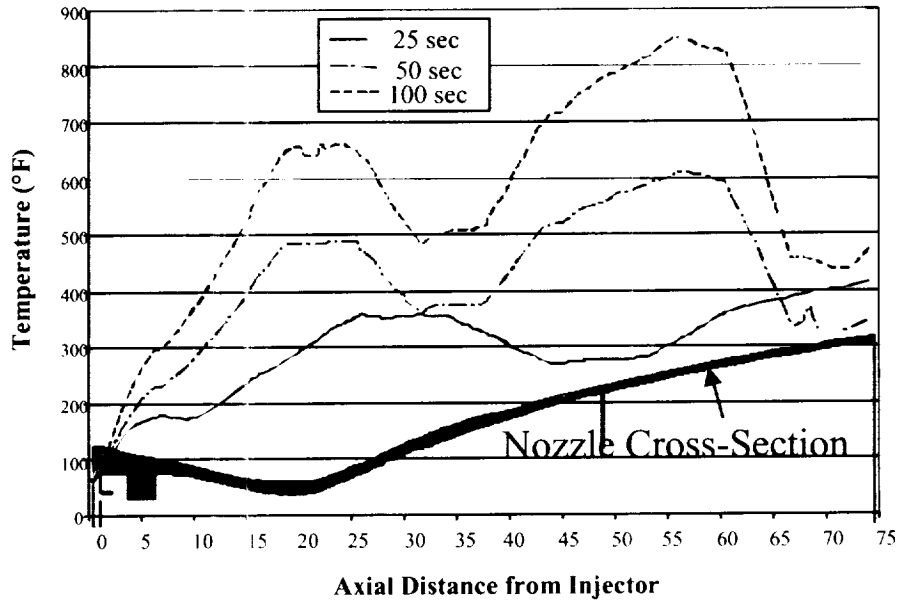


Figure 6. Nozzle Temperatures With Respect to Axial Location and Time

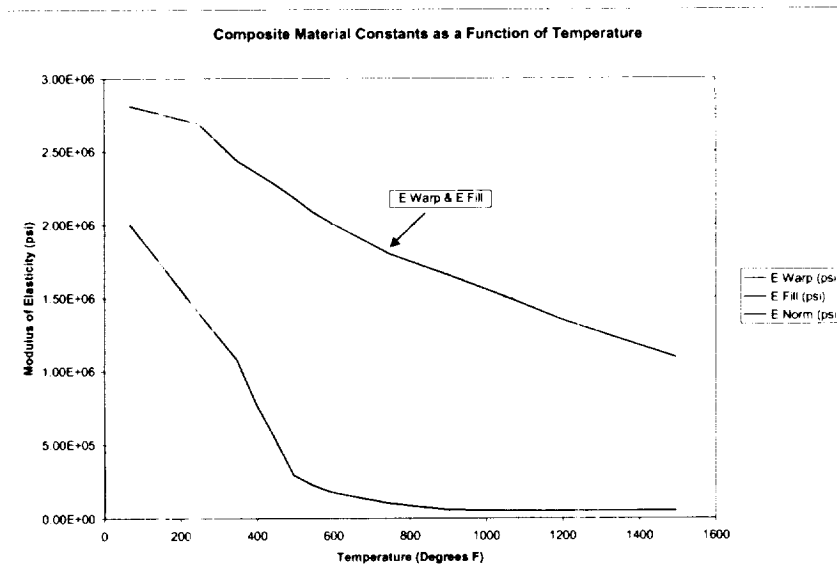


Figure 7. Composite Modulus of Elasticity Changes Based Upon Temperature

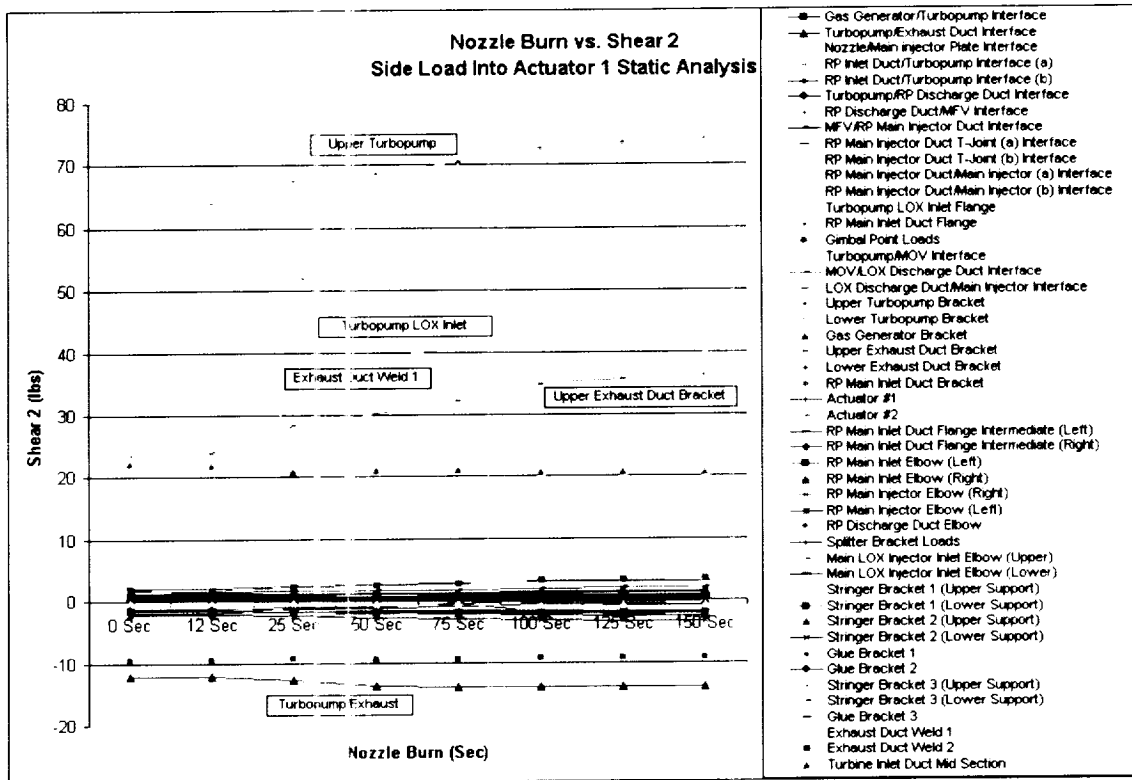


Figure 8. Side Load Into Actuator 1 Static Shear 2 Load vs. Nozzle Burn

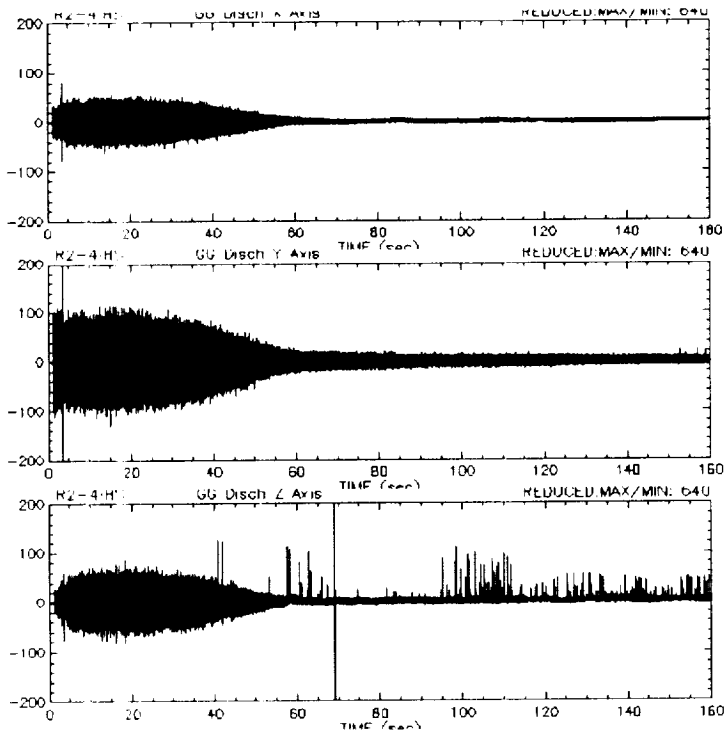


Figure 9. Gas Generator Accelerometer Data

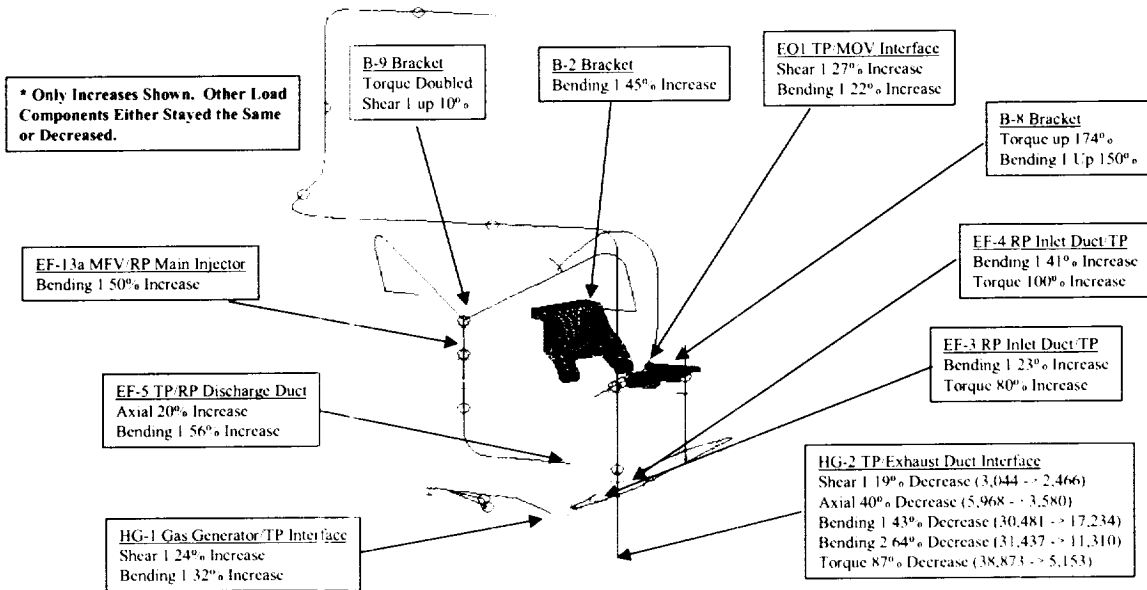


Figure 10. MC-1 60K Engine Finite Element Model Turbopump and Adjacent Components Load Path Change – Flight Loads Comparison – Nozzle Picture Excluded.

Random Vibration Engine System Response at 590 Hz

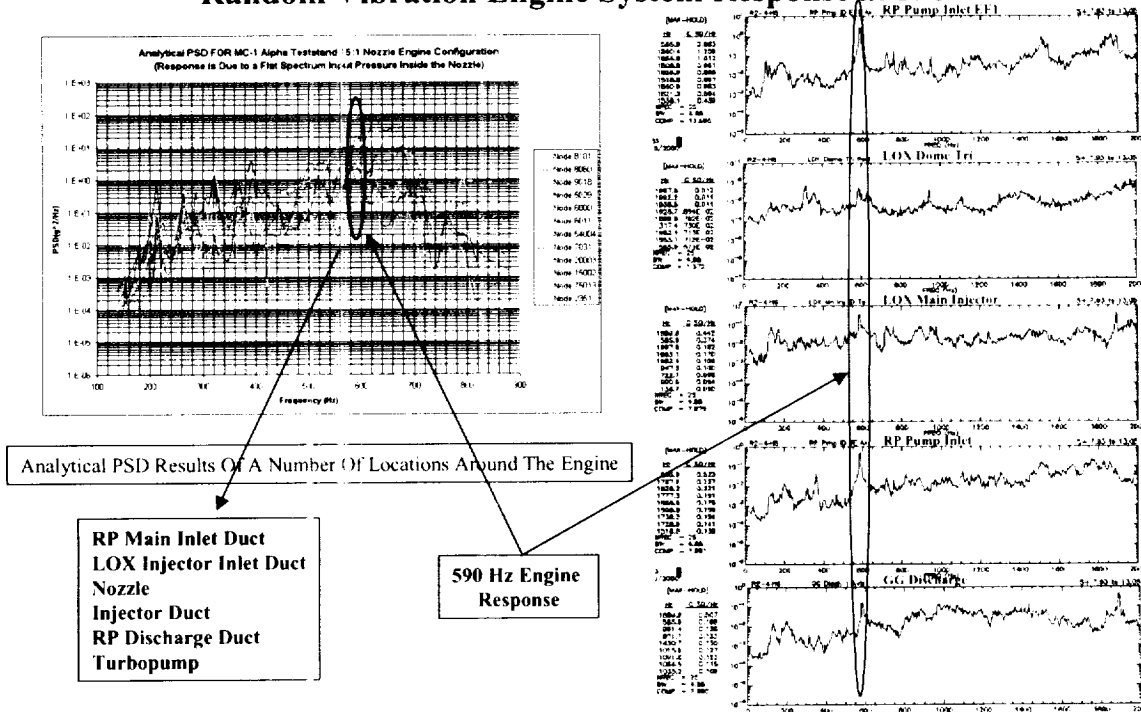
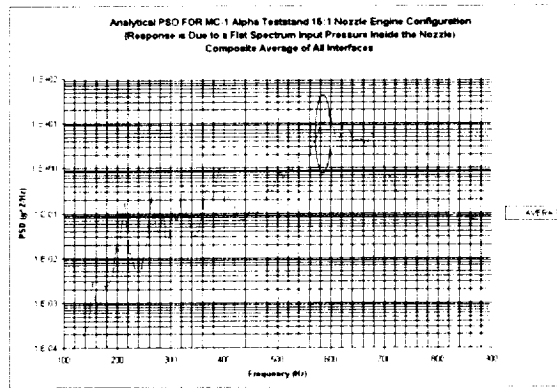


Figure 11. Random Vibration Engine Response at 590 Hz – Analytical Results Compared to Test Data From Various Components On the Engine – Nozzle Axial Mode at 596 Hz.



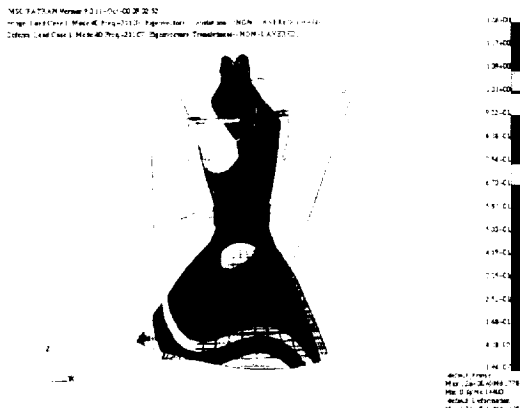
596 Hz Nozzle Axial Mode

- Shows 590 Hz Excitation Due to Random Environments
- Random Vibration Loads Methodology Refinement Needed
- Move From Component Analysis to A System Analysis



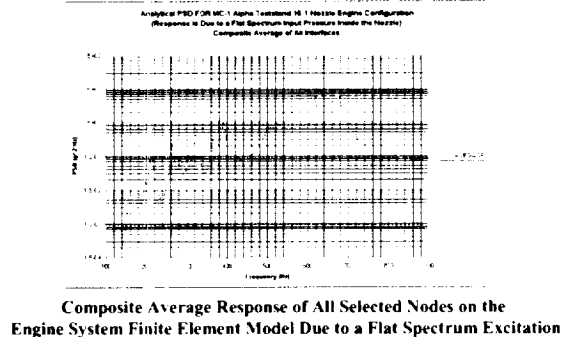
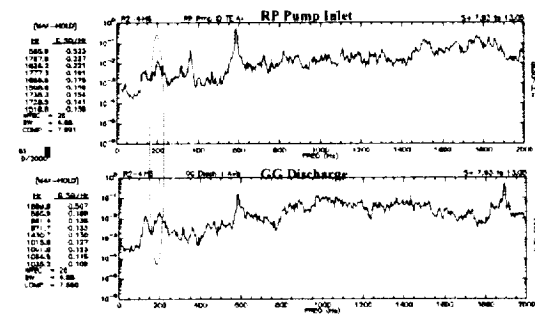
Composite Average Response of All Selected Nodes on the Engine System Finite Element Model Due to a Flat Spectrum Excitation

Figure 12. Random Vibration Model Response – 596 Hz Axial Mode of Nozzle Mode in Comparison with Figure 11 Test Data.



211 Hz Nozzle 1st Bending Mode

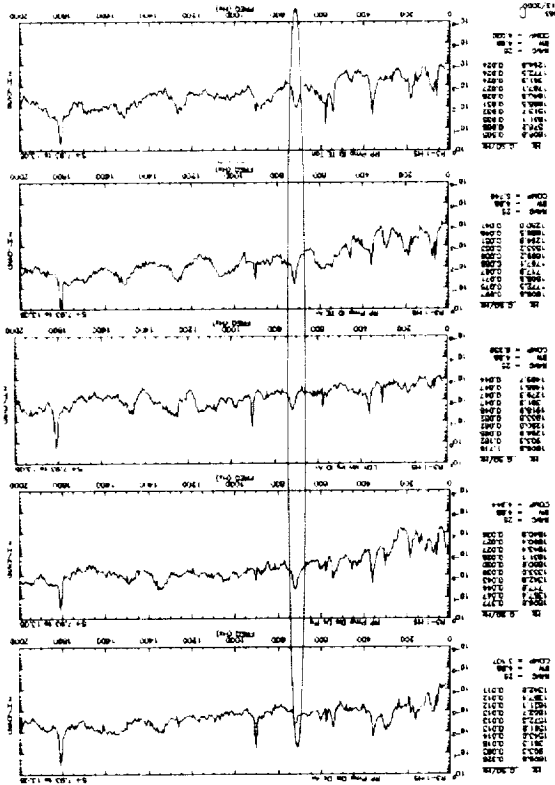
- Shows 205 Hz Excitation Due to Random Environments
- Random Vibration Loads Methodology Refinement Needed
- Move From Component Analysis to A System Analysis



Composite Average Response of All Selected Nodes on the Engine System Finite Element Model Due to a Flat Spectrum Excitation

Figure 13. Random Vibration Model Response – 211 Hz Analytical 1st Bending Mode Comparison to 205 Test Data Mode.

Figure 15. Random Vibration Engine Response – 725 Hz Nozzle/Pump Rocking Analytical Mode Comparison to 717 Test Data Mode



- Alpha Test Data Shows RP & LOX Duct Excitations
- Engine System Model Illustrates a Number of RP & LOX Duct Modes in the 700 Hz Region

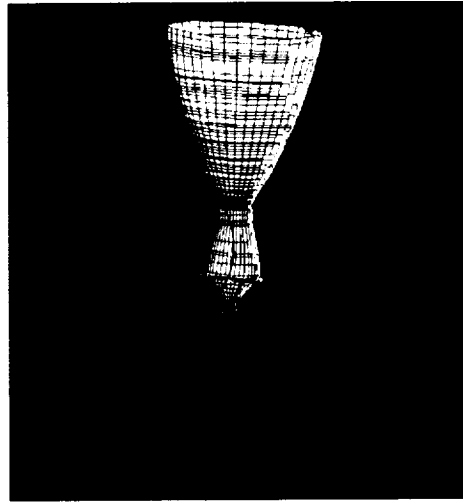


Figure 14. Random Vibration Engine Response – 57.4 Hz Analytical 2nd Nodal Diameter Mode Comparison to 58 Hz Test Data Mode.

